Mechanism study of 2-D laser array generation in a YAG crystal plate

Tao Zeng,[1] Jinping He,[2,3] Takayoshi Kobayashi,[2,3,4,5] and Weiwei Liu[1,6*]

[1]*Institute of Modern Optics, Nankai University, Key Laboratory of Optical Information Science and Technology, Ministry of Education, Tianjin 300071, China*
[2]*Advanced Ultrafast Laser Research Center, University of Electro-Communications, 1-5-1 Chofugaoka, Chofu, Tokyo 182-8585, Japan*
[3]*Japan Science and Technology Agency (JST), Core Research for Evolutional Science and Technology (CREST), 5 Sanbancho, Chiyoda-ku, Tokyo 102-0075, Japan*
[4]*Department of Electrophysics, National Chiao-Tung University, 1001 Ta Hsinchu Rd., Hsinchu 300, Taiwan*
[5]*Institute of Laser Engineering, Osaka University, 2-6 Yamada-oka, Suita, Osaka 565-0971, Japan*
[6]*Cooperative Innovation Centre of Terahertz Science, University of Electronic Science and Technology, Chengdu 611731, China*
[*] *liuweiwei@nankai.edu.cn*

Abstract: We have reproduced the process of two-dimensional array generation by using two crossing laser beams in a YAG crystal plate based on numerical simulation considering cross-phase modulation (XPM) and self-focusing. Furthermore, we come to the conclusion that both XPM and the cylindrical symmetry breaking in the initial beam profile contributes to the generation of two-dimensional array. In addition, we have studied the threshold input laser beam power for the two crossing beams splitting in a YAG crystal plate. Our study could be valuable in various applications, such as 2-D all-optical switching devices or multicolor pump-probe experiments.

OCIS codes: (320.2250) Femtosecond phenomena; (190.7110) Ultrafast nonlinear optics.

References and links

1. H. Crespo, J. T. Mendonça, and A. Dos Santos, "Cascaded highly nondegenerate four-wave-mixing phenomenon in transparent isotropic condensed media," Opt. Lett. **25**(11), 829–831 (2000).
2. J. Liu and T. Kobayashi, "Wavelength-tunable, multicolored femtosecond-laser pulse generation in fused-silica glass," Opt. Lett. **34**(7), 1066–1068 (2009).
3. J. Liu and T. Kobayashi, "Generation of microJ-level multicolored femtosecond laser pulses using cascaded four-wave mixing," Opt. Express **17**(7), 4984–4990 (2009).
4. M. Zhi and A. V. Sokolov, "Broadband coherent light generation in a Raman-active crystal driven by two-color femtosecond laser pulses," Opt. Lett. **32**(15), 2251–2253 (2007).
5. E. Matsubara, T. Sekikawa, and M. Yamashita, "Generation of ultrashort optical pulses using multiple coherent anti-Stokes Raman scattering in a crystal at room temperature," Appl. Phys. Lett. **92**(7), 071104 (2008).
6. H. Matsuki, K. Inoue, and E. Hanamura, "Multiple coherent anti-Stokes Raman scattering due to phonon grating in KNbO3 induced by crossed beams of two-color femtosecond pulses," Phys. Rev. B **75**(2), 024102 (2007).
7. K. Inoue, J. Kato, E. Hanamura, H. Matsuki, and E. Matsubara, "Broadband coherent radiation based on peculiar multiple Raman scattering by laser-induced phonon grating in TiO2," Phys. Rev. B **76**(4), 041101 (2007).
8. E. Matsubara, K. Inoue, and E. Hanamura, "Violation of Raman selection rules induced by two femtosecond laser pulses in KTaO3," Phys. Rev. B **72**(13), 134101 (2005).
9. J. Liu, J. Zhang, and T. Kobayashi, "Broadband coherent anti-Stokes Raman scattering light generation in BBO crystal by using two crossing femtosecond laser pulses," Opt. Lett. **33**(13), 1494–1496 (2008).
10. H. Zeng, J. Wu, H. Xu, and K. Wu, "Generation and weak beam control of two-dimensional multicolored arrays in a quadratic nonlinear medium," Phys. Rev. Lett. **96**(8), 083902 (2006).
11. J. Liu and T. Kobayashi, "Cascaded four-wave mixing and multicolored arrays generation in a sapphire plate by using two crossing beams of femtosecond laser," Opt. Express **16**(26), 22119–22125 (2008).
12. J. Liu, T. Kobayashi, and Z. Wang, "Generation of broadband two-dimensional multicolored arrays in a sapphire plate," Opt. Express **17**(11), 9226–9234 (2009).
13. J. P. He, J. Liu, and T. Kobayashi, "Tunable multicolored femtosecond pulse generation using cascaded four-wave mixing in bulk materials," Appl. Sci. **4**(3), 444–467 (2014).
14. A. Dubietis, G. Tamošauskas, G. Fibich, and B. Ilan, "Multiple filamentation induced by input-beam ellipticity," Opt. Lett. **29**(10), 1126–1128 (2004).

#241546 Received 25 May 2015; revised 9 Jul 2015; accepted 10 Jul 2015; published 15 Jul 2015

15. W. Liu and S. L. Chin, "Abnormal wavelength dependence of the self-cleaning phenomenon during femtosecond-laser-pulse filamentation," Phys. Rev. A **76**(1), 013826 (2007).
16. F. Silva, D. R. Austin, A. Thai, M. Baudisch, M. Hemmer, D. Faccio, A. Couairon, and J. Biegert, "Multi-octave supercontinuum generation from mid-infrared filamentation in a bulk crystal," Nat. Commun. **3**, 807 (2012).
17. L. Sudrie, A. Couairon, M. Franco, B. Lamouroux, B. Prade, S. Tzortzakis, and A. Mysyrowicz, "Femtosecond laser-induced damage and filamentary propagation in fused silica," Phys. Rev. Lett. **89**(18), 186601 (2002).
18. A. Dubietis, G. Tamošauskas, G. Fibich, and B. Ilan, "Multiple filamentation induced by input-beam ellipticity," Opt. Lett. **29**(10), 1126–1128 (2004).
19. D. Majus, V. Jukna, G. Valiulis, and A. Dubietis, "Generation of periodic filament arrays by self-focusing of highly elliptical ultrashort pulsed laser beams," Phys. Rev. A **79**(3), 033843 (2009).

1. Introduction

Recently, generation of ultrabroadband spectrum and ultrashort pulse through four-wave-mixing (FWM) process induced by the third-order susceptibility has attracted considerable interest. When two crossed femtosecond beams overlapping in time and space were synchronized in a piece of BK7 glass [1], a 1-D broadband multicolored side band array occurred, which was also observed in fused silica [2,3] and certain crystals such as PbWO4 [4], LiNbO3 [5], KNbO3 [6], TiO2 [7], KTaO3 [8], and BBO [9]. In addition, 2-D multicolored arrays were obtained in a quadratic nonlinear crystal [10] and sapphire plate [11,12].

The generation of 1-D multicolored sideband array can be explained by a cascaded four-wave-mixing process and the upshifted and downshifted sidebands correspond to the phase matching condition [1, 3]. But the explanation of the two-dimensional multicolored array generation using two crossed femtosecond laser beams in a sapphire plate or a quadratic nonlinear crystal hasn't been clear up to now. In this paper, we explored the mechanism of the 2-D multicolor arrays generated in the process of cascaded four-wave-mixing process based on numerical simulation, considering cross-phase modulation (XPM) and self-focusing under the pump of two noncol-linear cross-overlapped femtosecond beams. In addition, the threshold input laser beam power for the two crossing beams splitting in a YAG crystal plate has been studied numerically.

2. Numerical simulation model

We performed numerical simulation of the multicolored array generation in a YAG crystal plate by using two crossing femtosecond laser pulses according to the experimental conditions approximately [3,11–13]. The schematics of the expeirment is shown in Fig. 1.

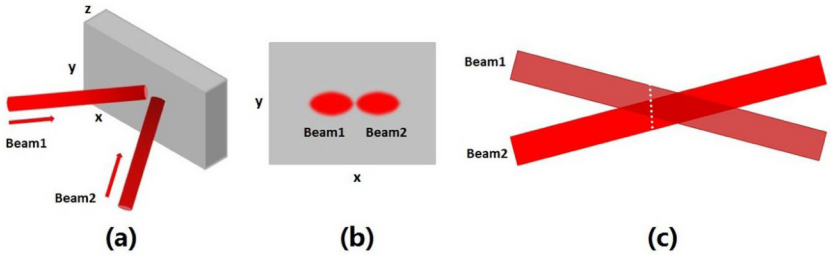

Fig. 1. Schematics of the simulation process. (a) Two laser beams were synchronously focused into a 1mm-thick sapphire plate with a crossing angle of 1.87°. (b) The cross section of the two beams on the surface of the sapphire plate. (c) longitudinal distribution of the two crossing laser beams in the y = 0 plane.

Femtosecond laser beam1 and beam2 were synchronously focused into a 1mm-thick YAG crystal plate as depicted in Fig. 1(a). And the YAG crystal plate was placed around the focus. The crossing angle between the two incident beams was about 1.87°. Figure 1(b) shows the cross section of the two elliptical beams on the surface of the YAG crystal plate and the diameter was about 500 μm for both beam1 and beam2 in the experiment. The two input laser beams were horizontal polarization with the repetition frequency of 1 KHz. The peak

#241546 Received 25 May 2015; revised 9 Jul 2015; accepted 10 Jul 2015; published 15 Jul 2015

wavelength of beam1 and beam2 was 800 nm and 700nm respectively. And The pulse duration of beam1 was 35 fs with an average power of 7 mW, while the pulse duration of beam2 was 60 fs. When the average power of beam2 was set to be 25 mW in the experiment which corresponded to a peak power of about 167 MW, the two beams started to split.

Since we mainly focus on the spatial distribution of the two crossing femtosecond laser beams in the YAG crystal, the temporal aspects of the propagation can be ignored. This processing method has been demonstrated to be valid by previous studies [14, 15]. Then we represent beam1 and beam2 as:

$$E_1 = A_1 e^{-i\omega_1 t + k_1 z} \text{ and } E_2 = A_2 e^{-i\omega_2 t + k_2 z} \tag{1}$$

where A_1 and A_2 denote the amplitude of the light field. ω_1 and ω_2 represent the frequency of beam1 and beam2. k_1 and k_2 denote the wave number of beam1 and beam2 respectively. The total field within the nonlinear medium is given by:

$$E = E_1 + E_2 \tag{2}$$

This field produces a three order nonlinear polarization within the medium, given by:

$$P = \varepsilon_0 \chi^{(3)} E^3 \tag{3}$$

With slowly varying amplitude approximation, we assume that the laser beam1 obeys the wave equation in the form:

$$2ik_1 \frac{\partial A}{\partial z} + \Delta_\perp A = -u_0 \omega_1 P^{NL}(\omega_1) \tag{4}$$

Then we can obtain $P^{NL}(\omega_1)$ from Eqs. (1)-(3) as follows:

$$P^{NL}(\omega_1) = \varepsilon_0 \chi^{(3)}(\omega_1, \omega_1, -\omega_1, \omega_1)\left[3A_1^2 A_1^*\right] + \varepsilon_0 \chi^{(3)}(\omega_1, \omega_2, -\omega_2, \omega_1)\left[6A_1 A_2^* A_1\right] \tag{5}$$

We introduce Eq. (5) into Eq. (4) and bring in the defocusing of plasma. Then the equation of the laser beam1 propagation in the nonlinear medium can be expressed as:

$$2ik_1 \frac{\partial A_1}{\partial z} + \Delta_\perp A_1 + \frac{2k_1^2}{n_1} \Delta n A_1 = 0 \tag{6}$$

where k_1 and n_1 denotes the wave number and refractive index of beam1 propagating in the sapphire plate respectively. Δn corresponds to the intensity dependent refractive index:

$$\Delta n = n_2 I_1 + 2n_2 I_2 - \alpha (I_1 + I_2)^m \tag{7}$$

The first item on the right hand of the above equation denotes the optical Kerr effect induced nonlinear refractive index and n_2 is 7×10^{-16} cm^2/W [16]. The second item refers to the nonlinear refractive index of beam1 induced by beam2 and reflects the cross-phase modulation process. The third item corresponds to the plasma defocusing effect-induced nonlinear refractive index and m is chosen to be 6, which is approximately the effective nonlinearity order of multiphoton ionization rate follows represent [17]. Here, α denotes an empirical parameter which gives rise to a clamped intensity of 5×10^{13} W/cm^2 in our simulation [17]. Note that different methods have been considered to taking into account the counteracting effect to the self-focusing, such as saturable nonlinear refractive index [18] or multi-photon absorption associated with plasma generation [19]. Saturable nonlinear refractive index model has the same effect as Eq. (7) without specifying the underlying physical mechanism which balances the self-focusing. Multi-photon absorption is crucial for

#241546 Received 25 May 2015; revised 9 Jul 2015; accepted 10 Jul 2015; published 15 Jul 2015

long propagation distance. Thus, plasma defocusing plays dominant role to balance the self-focusing, since in our case the thickness of our sample is much shorter than those used in [19].

Similarly, the wave equation of beam2 propagating in the sapphire plate can be written as:

$$2ik_2\frac{\partial A_2}{\partial z}+\Delta_\perp A_2+\frac{2k_2^2}{n_2}\left[n_2I_2+2n_2I_1-\alpha(I_1+I_2)^6\right]A_2=0 \tag{8}$$

Since in the experiment described by [11–13], two beams are centered at different wavelengths, i.e. 700 nm and 800 nm, we carried out numerical simulation of the two crossing femtosecond laser beams with the central wavelength of 700 nm and 800nm respectively based on the Eqs. (6) and (8) synchronously. It is worth mentioning if two beams are centered at the same wavelength, stimulated Raman scattering as observed in [11–13] will be suppressed. Besides, strong interference will take place between two beams with identical wavelength, resulting in intensity fringes. For the sake of saving computation time, during the simulation process we reduced the diameters of the two incident beams on the surface of the YAG crystal plate to 1/5 of those in the experiment and the input powers of the two beams were reduced to 1/25 in order to ensure the peak intensity remain the same. For beam1, the beam widths were 88 μm and 57 μm in the horizontal and vertical directions. And the beam widths of beam2 were 100 μm and 60 μm in the horizontal and vertical directions, respectively. The input powers of beam1 and beam2 were set to be 12 P_{cr} and 15 P_{cr} respectively. Pcr refers to the critical power for self-focusing and is defined as follows:

$$P_{cr}=3.77\lambda^2/\left(8\pi n_2 n\right) \tag{9}$$

where λ the laser wavelength, n_2 is the nonlinear refractive index and n refers to the refractive index.

3. Results and discussion

The simulation result is shown in Fig. 2. The elliptical initial profile of beam1 and beam2 is given by Figs. 2(a) and 2(b) respectively. Figure 2(c) shows the incoherent superposition of two laser beams intensity distribution in the horizontal plane of y = 0 when the two crossed laser beams propagates through a 1-mm YAG crystal plate. Multiple strips could be clearly observed in Fig. 2(c). Each strip indeed represents one filament induced by the dynamic interplay between the Keff effect induced self-focusing and plasma defocusing [17–19]. At the output plane of the crystal, multiple filaments are observed as multiple laser spots. Therefore, Figs. 2(d)-2(i) depict evolution of the beam profile at different propagation distances until 2-D laser array is observed. In details, Fig. 2(d) represents the transverse intensity distribution at z = 0.5 mm, which indicates the self-focusing process of the two elliptical laser beams in the YAG crystal. The two laser beams intersects at a distance of 0.5 mm in the plate as shown in Fig. 2(d). And then both two beams start to split. Figure 2(e) shows that a one-dimensional array has been formed at the distance of 0.6 mm. With the increase of the propagation distance, beam1 and beam2 starts to split on the vertical direction as is shown in Fig. 2(f). Figure 2(g) indicates that a two-dimensional array with three rows and two columns has appeared apparently. Further, with the increase of the propagation distance, more columns have come up as is shown in Figs. 2 (h) and 2(i).

As the spatial asymmetric distribution of the initial input pulse could lead to the beam breakup [18, 19], the ellipticity of the initial laser beams plays an important role in the formation of two-dimensional array. More importantly, XPM significantly enhances the asymmetry of the pulse's phase front when two beams cross each other at an angle. As indicated in Fig. 1(c), across the dotted white line, which is parallel to x-axis, the upper part of the beam2 suffers stronger phase modulation than the bottom part because of XPM. However, this asymmetry does not occur along y-axis. The same phenomenon happens to beam1 as well. Hence, due to XPM, the cylindrical symmetry of the pulse phase will broken no matter if the initial beam profile is elliptic or not. One would expect that the enhanced asymmetry

#241546 Received 25 May 2015; revised 9 Jul 2015; accepted 10 Jul 2015; published 15 Jul 2015

will lower down the power required to generate a 2D laser array. Then we can draw a conclusion that the formation of two-dimensional array was induced by both cross-phase modulation (XPM) and cylindrical symmetry breaking in the initial beam profile.

In addition, we have studied the threshold initial power for the laser beams splitting in a YAG crystal plate by using two crossing femtosecond laser pulses based on simulation. We carried out the same simulation process with different input power of beam2. The input peak power of beam1 was set to be 8.5 P_{cr} and the input peak power of beam2 was set as 5, 10 and 15 times the critical power for self-focusing, respectively.

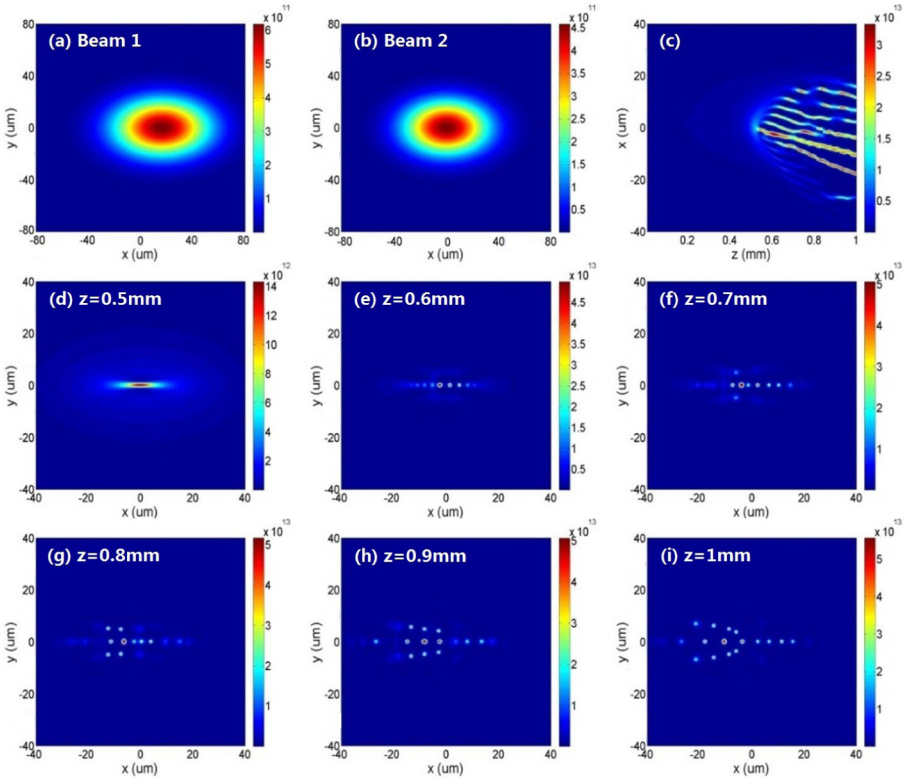

Fig. 2. Simulation result with two crossing elliptical laser beams. (a) and (b) pattern of input beam1 and beam beam2, (c) longitudinal laser intensity distribution in the y = 0 plane and transverse intensity distribution at (d) z = 0.5 mm, (e) z = 0.6 mm, (f) z = 0.7 mm, (g) z = 0.8 mm, (h) z = 0.9 mm, (i) z = 1 mm.

In Fig. 3, the laser intensity distributions obtained in a YAG crystal by using two crossing laser beams are depicted for different input power values of laser beam2. Figures 3(a), 3(b), and 3(c) illustrate the longitudinal intensity distribution at three different input peak powers of beam2, while Figs. 3(d), 2(e), and 2(f) show the corresponding laser intensity cross-section patterns at the propagation distance z = 1 mm on the exit surface of the crystal plate.

When the input laser power of beam2 is 5 times the critical power for self-focusing, it can be seen that only a single spot has been formed on the cross section at the propagation distance of 1mm. Only single filament is found in Fig. 3(a), while multiple filaments are generated in Figs. 3(b) and 3(c) similar to Fig. 2(c). As the input laser power of beam2 increases to 10 P_{cr}, it is clear that the two laser beams starts to split at the distance of z = 0.8 mm and one-dimensional array has been formed on the exit surface the YAG crystal plate. When the input laser power of beam2 is 15 P_{cr}, it can be seen that the number of spots in the x direction increases and the beams start to split in the y direction.

#241546 Received 25 May 2015; revised 9 Jul 2015; accepted 10 Jul 2015; published 15 Jul 2015

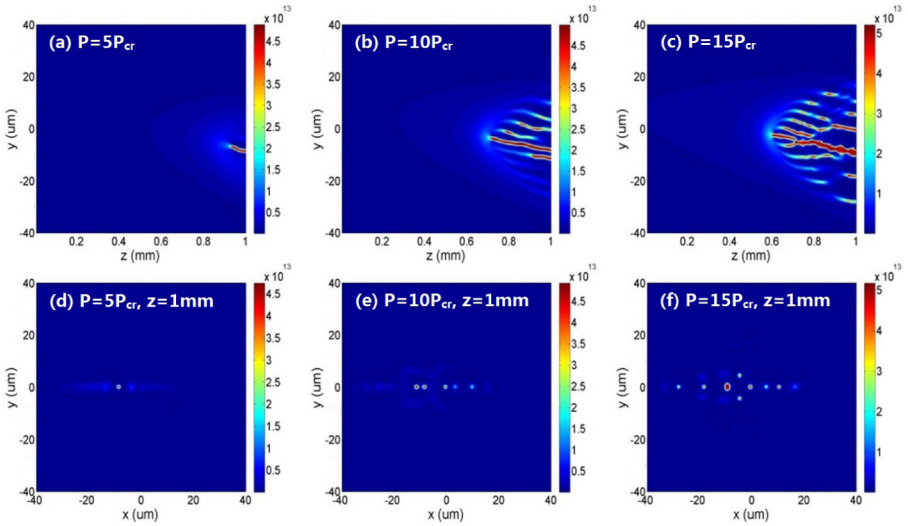

Fig. 3. Simulatied longitudinal laser intensity distribution in the y = 0 plane and cross section with two crossing elliptical laser beams when the input laser power of beam2 is set as (a) and (d) P = 5 Pcr, (b) and (e) P = 10 Pcr, (c) and (f) P = 15 Pcr.

Finally we come to the conclusion that the threshold input power of beam2 for the laser beam splitting is about 10 P_{cr} which corresponds to a peak power of about 181 MW. This result keeps consistent with that in the experiment [11–13]. According to the previous discussion, it could be foreseen that if one could further enhance the asymmetry of XPM caused phase modulation, such as increasing the crossing angle or the ellipicity of the initial beam profile, offset the beam in y-axis and so on, the threshold power required to generate 2-D laser array could be even lower.

4. Conclusion

In summary, we have reproduced a two-dimensional laser array by using two crossing elliptical laser beams in a YAG plate based on numerical simulation considering cross-phase modulation (XPM) and self-focusing. We come to the conclusion that both XPM and the cylindrical symmetry breaking in the initial beam profile contributes to the generation of two-dimensional laser array. In addition, we have studied the threshold input laser beam power for the two crossing beams splitting in a YAG crystal plate. Our study could be valuable in various applications, such as 2-D all-optical switching devices or multicolor pump-probe experiments.

Acknowledgment

This work is financially supported by National Basic Research Program of China (2014CB339802, 2011CB808100) and National Natural Science Foundation of China (11174156). W.L. acknowledges the support of the open research funds of State Key Laboratory of High Field Laser Physics, Shanghai Institute of Optics and Fine Mechanics (SIOM). And fruitful discussion with Prof. Y. Cheng in SIOM is appreciated.

#241546 Received 25 May 2015; revised 9 Jul 2015; accepted 10 Jul 2015; published 15 Jul 2015